Electronic Supplementary Material (ESI) for Physical Chemistry Chemical Physics.

Supporting Information

Distance measurements between manganese(II) and nitroxide spin-labels by DEER determine a binding site of Mn^{2+} in the HP92 loop of ribosomal RNA

Ilia Kaminker[+] , Morgan Bye[+], Natanel Mendelman[+], Kristmann Gislason,[#] Snorri Th. Sigurdsson[#] and Daniella Goldfarb[+]*

[+]*Department of Chemical Physics, Weizmann Institute of Science, Rehovot 76100, Israel.* [#]*University of Iceland, Department of Chemistry, Science Institute Dunhaga 3, 107 Reykjavik, Iceland.*

Sample preparation.

All reagents, unless mentioned otherwise, were purchased from Sigma and used without further purification.

RNA preparation: All RNA constructs were purchased from Dharmacon in the 2'-ACE protected form and deprotected according to the vendor's protocol. The spin labeling reaction (See Fig. 1b) was performed according to the published protocol.[1-2] Briefly the 2' amino modified RNA constructs were reacted at -8 °C in a formamide / DMF / 70 mM boric acid buffer, pH 8.6 mixture with an 15x – 20x excess of 4-isocyanato-TEMPO (Toronto Research Chemicals, Canada) dissolved in dry DMF. Subsequent aliquots of fresh 4-isocyanato-TEMPO were added after one and two hours of the reaction. The reaction was stopped after 3 hours by the addition of a formamide loading buffer to a final v/v ratio of 0.75/0.25 formamide / reaction mixture. The resulting mixture was loaded on a denaturating polyacrylamide (18% (19:1 acryladmide : bisacrylamide), 8M urea) gel and purified by cutting a single band. The purified RNA was eluted overnight in 0.5 M ammonium acetate; 1 mM EDTA buffer. then extracted with phenol, precipitated with 70% ethanol, dried in SpeedVac vacuum centrifuge and stored as dry powder at -20 °C until use. More details are given in [3].

EPR sample preparation: Monolabeled 33bp RNA constructs were mixed with 1.5 fold excess of the 11bp complimentary strand (See Fig. 1a in the main text) in the RNA folding buffer (50 mM HEPES, 100 mM NaCl, 30% (v/v) d_3-glycerol (Cambridge Isotopes) in D_2O pH 7.5) and folded by cooling gradually for 3 hours from 95°C to room

temperature. 360 μM $MnCl_2$ solution in 60% (v/v) d3 – glycerol was added to the folded RNA to obtain a final sample composition of 135 μM RNA / 135μM $MnCl_2$, 31mM HEPES / 62mM NaCl, 41% d3-glycerol in D_2O. In the sample for X-band CW EPR Mn^{2+} was omitted and the sample was diluted by 60% d3 – glycerol in D_2O (v/v) to the same final RNA concentration.

The doubly labeled RNA construct RNA(3,31) was prepared in the same manner as the monolabeled constructs omitting the addition of the $MnCl_2$. The final sample composition was 166 μM RNA / 33 mM HEPES / 66 mM NaCl / 33% d3-glycerol in D_2O.

All EPR samples were thoroughly mixed by pipetation, incubated for approximately 5 min on ice and loaded into W-band EPR tubes (ID 0.64 mm, OD 0.8 mm). X-band CW EPR spectra of the nitroxide labeled RNA were measured for all the samples immediately following their preparation. The samples were then frozen in liquid nitrogen and stored immersed in liquid nitrogen until measured by pulsed EPR.[3]

CW X-band EPR measurements

X-band (9.5 GHz) CW EPR measurements were performed on a Bruker ELEXSYS 500 spectrometer using two round quartz capillaries (0.6 i.d. × 0.84 o.d., VitroCom Inc.). The total sample volume was ~ 6-7 μl. The temperature was 310 K, modulation amplitude 0.2 mT, time constant 655 ms and sweep time 167 s. The spectra shown were normalized to the maximum intensity to ease comparison.

X-band CW EPR spectra of the RNA(31) and RNA(3) without Mn^{2+} are shown in Fig. S1. The spectra of both RNA constructs exhibit an EPR spectrum characteristic of a nitroxide spin label with a significant motional freedom.

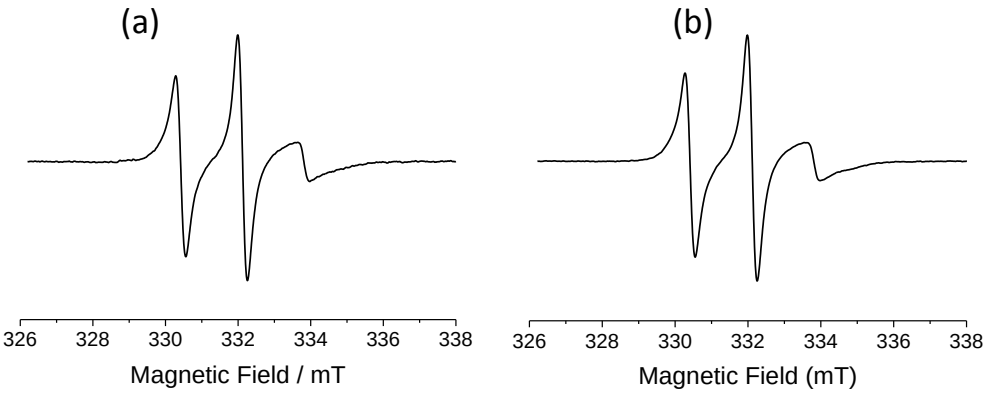

Figure S1. X-band CW EPR (310 K) spectra of the (a) RNA(31) and (b) RNA(3)

W-band pulsed EPR experiments

W-band pulse EPR experiments were performed on a home built EPR spectrometer.[4] The frozen EPR samples were loaded into the EPR probehead while immersed in liquid N_2 bath and then the entire cold probe was transferred to the precooled cryostat. Experimental parameters are given in the relevant sections.

Field Swept Echo Detected EPR Spectra

W-band Echo detected EPR spectrum of RNA(3,31) is shown on Fig. S2a. Experimental parameters were $\pi/2$, π = 60ns / 120ns; τ =550ns ; repetition time was 5ms; temperature was 40K.

Echo-detected EPR spectra of Mn^{2+} / RNA(3) complex, which show the Mn^{2+} $|-1/2,M_I\rangle \rightarrow |1/2,M_I\rangle$ central transitions and the nitroxide signals, are presented in Figs. S2b,c. Because of the larger transition probability of the Mn^{2+} central transitions compared to that of the nitroxide, different microwave (MW) power settings are required for maximizing each of the signals. The spectrum shown in Fig. S2b was recorded with a MW power optimized for $\pi/2$, π (60ns / 120ns)pulses for the Mn^{2+} $|-1/2,M_I\rangle \rightarrow |1/2,M_I\rangle$ transitions and consequently the nitroxide signal, marked with an arrow in Fig. S2b, is barely visible. The spectrum shown in Fig. S3c was acquired with a MW power optimized for pulses of $\varphi = \sim\pi/2$ and $2\varphi = \sim\pi$ (60ns / 120ns) for the nitroxide, yielding $\varphi = \sim 3/2\pi$ and $2\varphi = \sim 3\pi$ for the Mn^{2+} central transitions. This generates a spectrum with a clear contribution of the nitroxide, while the Mn^{2+} spectrum appears inverted. Under

these conditions it is straightforward to set the pump pulse on the nitroxide signal for the DEER experiment. τ =550ns; repetition time was 50ms; temperature was 10K.

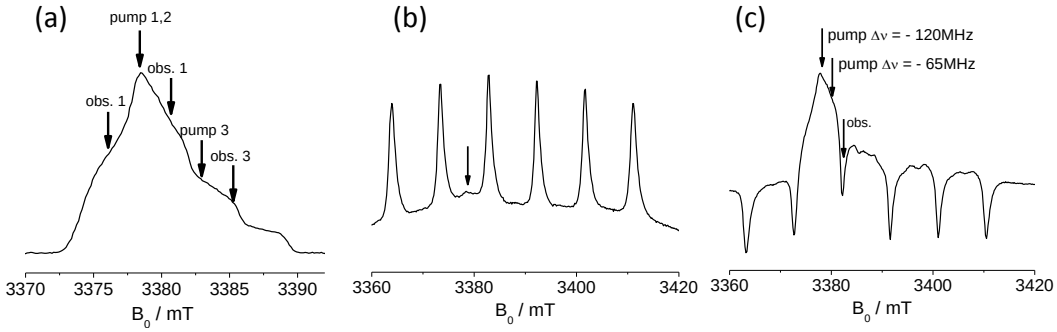

Figure S2. ED-EPR spectra of (a) RNA(3,31) and of Mn^{2+} / RNA(3) with mw power optimized for observation of Mn^{2+} (b) and with mw power optimized for observation of the nitroxide (c). Arrows in (a,c) indicate pulse positions for the DEER experiments presented in the main text. Red arrow in (b) indicate the position of the "barely visible" nitroxide signal.

Distance measurements of doubly labeled RNA(3,31)

W-band DEER measurements on RNA (3,31) were performed with the pulse sequence $\pi/2_{obs}-\tau_1-\pi_{obs}-t-\pi_{pump}-(\tau_1+\tau_2-t)-\pi_{obs}-\tau_2-$echo.[5] The echo was measured as a function of t, while τ_2 and τ_1 were kept constant. DEER traces were summed over eight τ_1 values starting with 350 ns and a step of 12.5 ns and an 8 step phase cycle was implemented to suppress hardware artifacts and pulse imperfections ($\pi/2_{obs}$ +x,-x,+x,-x,+x,-x,+x,-x; π_{obs} +x,+x,+x,+x,-x,-x,-x,-x; π_{pump} +y,+y,-y,-y,+y,+y,-y,-y; π_{obs} +x,+x,+x,+x,+x,+x,+x,+x; receiver a,-a,a,-a,a,-a,a,-a) The temperature was 40 K and the repetition time was 5 ms. For all DEER measurements described in the main text the pump frequency was 94.9 GHz tuned to the center of the cavity bandwidth, the pump pulse was 25 ns for all measurements. For measurements designed as 1,2 in Fig. 2, main text, the magnetic field was set to 3378.4 mT (the maximum of the nitroxide spectrum) and 3383 mT for experiment 3. The observer frequency was set to 94.835 GHz for experiments 2,3 with observer pulses of 60/120 ns for $\pi/2$ / π pulses, respectively. For

experiment 1 the observer frequency was 94.965 GHz, and the observer pulses were 70/140 ns. Distance distributions were obtained by fitting time domain traces with a distance distribution of a single Gaussian using the DeerAnalysis software package[6]. The raw DEER data are presented in Figure S3a.

W-band Mn^{2+} - nitroxide DEER experiments.

W-band Mn^{2+} - nitroxide DEER measurements were performed as described above for the nitroxide-nitroxide distance measurements but with different parameters. The temperature was set to 10 K. The observer frequency was set to the 3rd hyperfine line of the Mn^{2+} spectrum, corresponding to a magnetic field of 3378.4 mT for 94.78 GHz and 3380.5 mT for 94.835 GHz. The durations of the observer pulses were 40/80 ns, with a power set to produce $\pi/2$ and π pulses for the Mn^{2+} central transitions. The pump pulse frequency was always set to 94.9 GHz, which corresponded to pumping at the maximum of the nitroxide spectrum for B=3378.4 mT and to B=3380.5 mT for its position in the g_{zz} region. The pump pulse duration was 25 ns with a power set to produce a π pulse for nitroxide spins. The repetition time was 1 ms. Distance distributions were obtained by fitting a single Gaussian for the RNA(3) measurements and two Gaussians for the RNA(31) measurements. Adding the 2nd Gaussian to the RNA(3) data did not result in significant improvement of the fit and the best fit results were highly dependent on the initial parameters. The raw DEER data are presented in Figures S3b,c.

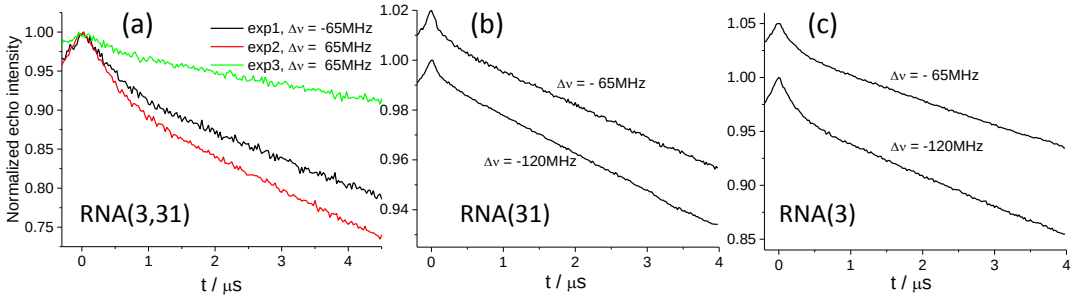

Figure S3. Raw DEER traces of (a) RNA(3,31), (b) Mn^{2+}/RNA(31), (c) Mn^{2+}/RNA(3). In (b) and (c) the upper traces are shifted for clarity.

Comparison between Gaussian fitting and Tikohonov regularization

Distance distributions obtained using Tikohonov regularization option of DeerAnalysis are presented in Figs S3b,d for Mn^{2+}/RNA(3) and Mn^{2+}/RNA(31), respectively. The corresponding fits overlaid with the experimental data after background subtraction are presented on Figure S4a,c. For both experiments performed on RNA(3) the resulting distance distribution is very broad and covers distances from 2 to 6 nm, we therefore decided it is better represented as a broad Gaussian as was shown in the main text. For the DEER data obtained for RNA(31) the distance distributions show a pronounced peak centered at (2.3-2.4) nm superimposed on other distances, again covering distances up to 6 nm. It is well know that Tikohonov regularization is not a good way to obtain a distance distribution when two distances with markedly different distribution width are present in the same data. We thus decided to represent such a distribution as a sum of two Gaussians as was presented in the main text. It is important to note that the width of the peak centered at 2.3-2.4 nm is essentially defined by the choice of the regularization parameter α=100, again supporting the notion that it is rather narrow.

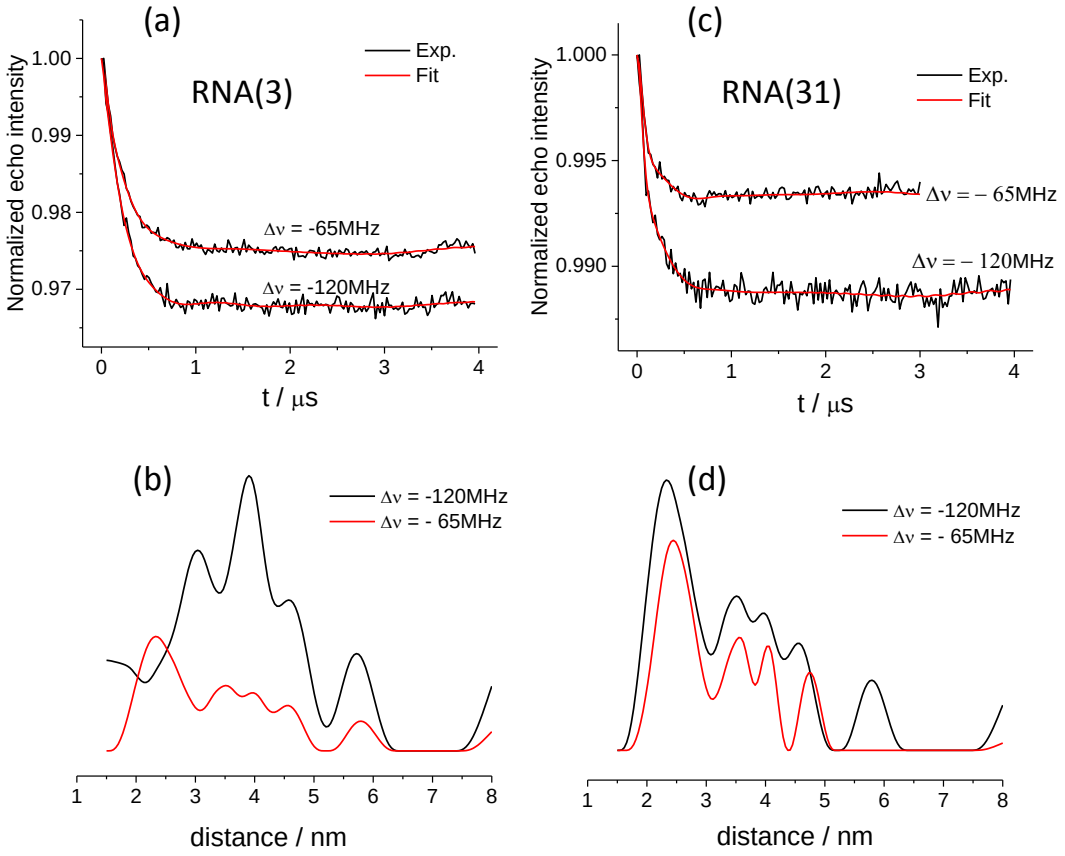

Figure S4. W-band DEER traces after background removal of (a) Mn^{2+}/RNA(3) and (c) Mn^{2+}/RNA(31) and the fits (red traces) obtained with distance distributions shown in b, d, obtained with Tikhonov regularization.

Experimental considerations for the Mn^{2+} - NO DEER measurements.

In DEER distance measurements between two different paramagnetic centers there is a choice of which center to use as the observer and the pump spins. In general we want to maximize S/N ratio, which is proportional to λV_0 where λ is the modulation depth and V_0 is echo intensity of the observer spins at the observer frequency. The MW field amplitude is given by $\omega_1=\gamma B_1[S(S+1)-M_s(Ms+1)]^{1/2}$ and therefore effective ω_1 frequency for the given MW power is different for the Mn^{2+} (S=5/2) central transitions and the nitroxide (S=1/2) , with $\frac{\omega_{1(Mn^{2+})}}{\omega_{1(SL)}}=3$. It is therefore possible to obtain shorter π pulses and broader excitation bandwidth for Mn^{2+} (S=5/2) with a given MW power. The shortest π pulse available on our spectrometer is 25 ns for S = 1/2 and ~ 12.5 ns for S=5/2. (The deviation

from 3 is due to limitations in the response time of the MW pin attenuators). As the nitroxide spectrum is significantly narrower than that of the Mn^2 it is preferable to use nitroxide spins as pumped spins and observe the Mn^{2+}. In addition the signal intensity of the Mn^{2+} central transition is larger than for the nitroxide. Moreover, since only the observer spins are required to be at thermal equilibrium for DEER experiment this experimental configuration has an additional advantage because of the shorter T_1 of the Mn^{2+}. This allows increasing the repetition rate and thus expedites data accumulation.

Finally one has to consider the echo decay rate, or the so called phase memory time, T_M. Here we strive for a long T_M for the observer spins. The phase memory time of Mn^{2+} at 10 K is comparable to that of the nitroxide.

Modelling

Any bases in our RNA model differing from those in the crystal structure were mutated using the 3DNA mutate_bases function[7] such that the bases could be changed and optimized without affecting the ribose-phosphate backbone. 2' nitroxide spin labels were built manually in a manner similar to that outlined for MTSL in MtsslWizard[8] by addition of atoms to the model, then automatic addition of any missing protons to the model and bond length and angle optimization using Swiss-PdbViewer GROMOS 43B1 force field.[9] Chi-angles in the spin labels were then randomly generated and checked for clashes of label conformations with the assumed static RNA, as well as clashes between the spin label atoms, where a clash is defined as a violation of a Van der Waals cutoff (3.4 angstroms). Mn^{2+} addition to the model was made using Coot's[10] building tool for adding atoms. The RNA backbone was fixed in Swiss-PdbViewer and a hydrogen bond network built between nucleotides and metal ion before hydrogen bond energy optimization was conducted, using the GROMOS 43B1 force field to optimize metal placement.

References

1. T. E. Edwards, T. M. Okonogi, B. H. Robinson, S. T. Sigurdsson, *J. Am. Chem. Soc.* **2001,** *123* (7), 1527-1528.
2. T. E. Edwards, S. T. Sigurdsson, *Nature Protocols* **2007,** *2* (8), 1954-1962.
3. I. Kaminker , Goldfarb, D. in Methods in Molecular Biology : RNA Remodeling Proteins methods and protocols, Ed. Marc Boudvillain, Springer New York Heidelberg Dordrecht London: 2014, Chapter 10, 137-164

4. D. Goldfarb, Y. Lipkin, A. Potapov, Y. Gorodetsky, B. Epel, A. M. Raitsimring, M. Radoul, I. Kaminker, *J. Magn. Reson.* **2008,** *194*, 8-15.
5. M. Pannier, S. Veit, A. Godt, G. Jeschke, H. W. Spiess, *J. Magn. Reson.* **2000,** *142*, 331-340.
6. G. Jeschke, V. Chechik, P. Ionita, A. Godt, H. Zimmermann, J. Banham, C. R. Timmel, D. Hilger, H. Jung, *Appl. Magn. Reson.* **2006,** *30* (3-4), 473-498.
7. L. Xiang-Jun, W. K. Olson, *Nucleic Acids Research* **2003,** 5108-5121.
8. G. Hagelueken, R. Ward, J. H. Naismith, O. Schiemann, *Appl. Magn. Reson.* **2012,** *42* 377- 391.
9. W. R. P. Scott, P. H. Hunenberger, I. G. Tironi, A. E. Mark, S. R. Billeter, J. Fennen, A. E. Torda, T. Huber, P. Kruger, W. F. van Gunsteren, *J. Phys. Chem. A* **1999,** *103* , 3596-3607.
10. http://www.ncbi.nlm.nih.gov/pubmed/15572765/